

中国科学院
近代物理研究所

年報

ANNUAL REPORT 1985

Institute of Modern Physics

Academia Sinica

科学技术文献出版社重庆分社

1986·5

中国科学院近代物理研究所 (1985) 年报

中国科学院近代物理研究所年报编委会	编 辑
科学技术文献出版社重庆分社	出 版
重庆市市中区胜利路132号	
新华书店重庆发行所	发 行
科学技术文献出版社重庆分社印刷厂	印 刷

开本: 787×1092毫米1/16	印张: 9.75	字数: 25万
1986年11月第一版	1986年11月第一次印刷	
科技新书目: 135—266	印数: 1600	

统一书号: 13176·151

定价: 2.50元

FOREWORD

This annual report covers scientific research and progress of HIRFL project carried out in Institute of Modern Physics, Academia Sinica during the year 1985.

29 scientific papers published in this report are concerning to the theoretical nuclear physics and experimental nuclear physics with heavy ions. Among them, I would like to point that new data of the deep inelastic collision of the light nuclear systems ($^{14}\text{N} + ^{27}\text{Al}$, ^{40}Ca , ^{58}Ni) enable us to study the dependence of the characteristics of DIC on the bombarding energy and the projectile, the structure effect of DIC and the relation of DIC with Alpha particle emission etc. All these interesting results inspire us to carry on further investigation such as incomplete deep inelastic collision in this field.

The research on application of nuclear technique has been performed by using the 600 KV high voltage equipment and the heavy ion implantater. $2 \times 2\text{MV}$ tandem electrostatic accelerator designed by IMP has extracted its first proton beam on September 18, 1985. This machine will be mainly used for applied researches on PIXE and mass spectroscopy as well. Technical service to national economy such as content monitor of crude petroleum etc. has primarily got cost benefit.

During the year 1985, construction of HIRFL project was progressing steadily as before. The assembling of injector SFC and its magnetic field measurement have been finished. The beam tuning will be started after rf conditioning with required vacuum. The lower yokes of sector magnets of SSC have been mounted on sites. The finishing work of the monolithic vacuum chamber has been completed by special designed tools after welding together of 8 pieces in the accelerator hall. Fabrication of remaining parts of SSC is now under way.

The design of 8 experimental equipments at the beam line terminals of HIRFL has been partly finished and ordered from Chinese factories. The design of beam line from SSC to the terminals is also under progressing.

From August 13 to 17, 1985, the Third Chinese Comestic Workshop on Heavy Ion Physics was held in our Institute. During the meeting, 34 Chinese physicists from institutes and universities presented 22 scientific papers.

The Director of Institute of Modern
Physics, Academia sinica

中国科学院近代物理研究所年报（1985年）

顾 问：杨澄中

主 编：魏宝文

副主编：张恩厚、邬恩九

编辑部成员：（以姓氏笔划为序）

王树芬、刘建业、乔庆文、闵 亚、李文新、

周智明、诸永泰、蒋西虹、戴光羲

CONTENTS

1. Theoretical Nuclear Physics	
1-1	Mass Drift in Heavy Ion Reaction (3)
1-2	Mass Dissipation Process in Heavy Ion Collisions (4)
1-3	A Study on DIC by Heavy Ions (5)
1-4	The Dependence of the Energy and Mass on the Condensation Probability γ_β in the Complex Particle Emission Probability..... (6)
1-5	Temperature-Dependent Optical Potential and Mean Free Path Based on Skyrme Interactions (8)
1-6	Structure of Quasic-Molecule in Heavy Ion Reactions..... (9)
1-7	A Mean Field for the Fission of Heavy Nuclei..... (10)
1-8	The Description of Fission Deformation by Cassinian Ovaloid..... (11)
1-9	A Discussion on Process of Asymmetric Fission..... (13)
1-10	On the $i_{13/2}$ -Neutron Pair in the Pt Isotopes..... (14)
2. Experimental Nuclear Physics	
2-1	Evidence for two Emission Modes of Emitted α -Particles in Low Ener- gy ^{12}C Induced Reactions..... (17)
2-2	Surprisal Analyses for Spectra in HI Transfer Reaction..... (18)
2-3	Research of Quasi-Elastic and Inelastic Scattering Induced by 92MeV and 76MeV ^{14}N on ^{27}Al Target..... (19)
2-4	Diffusion Model Analysis of $^{14}\text{N} + ^{\text{nat}}\text{Ca}$ Dissipative Collision..... (20)
2-5	A Study on $^{14}\text{N} + \text{Ni}$ Reaction at 94.2MeV..... (22)
2-6	Light Particle Emission in $^{12}\text{C} + ^{64}\text{Ni}$ Reaction..... (23)
2-7	A Macroscopic Analysis for Most Probable Energy of Light Particle Pro- duct..... (24)
2-8	Measurements of Cross Section Angular Distribution for Residues in Reaction $^{12}\text{C} + ^{93}\text{Nb}$ (26)
2-9	The Structure of the Complete Fusion Excitation Function on $^{12}\text{C} + ^{28}\text{Si}$ Reaction..... (27)
2-10	Model Analysis of the Complete Fusion Excitation Function of ^{12}C + ^{28}Si System..... (28)
2-11	Relaxation Time of Mass Drift Mode..... (29)
2-12	Two Kinds of Quasi-Fission Induced by ^{238}U (31)
2-13	Simulation of Quasi-Fission Reaction Induced by ^{238}U (32)
2-14	The $^{31}\text{S} + ^{100}\text{Mo}$ Reaction at $E = 150\text{MeV}$ (34)
2-15	Element Distribution for the Reactions $^{32}\text{S} + ^{100}\text{Mo}$, $^{32}\text{S} + ^{93}\text{Nb}$ and $^{28}\text{Si} + ^{93}\text{Nb}$ near the Coulomb Barrier..... (35)
2-16	Fusion Reaction between ^{32}S and $^{24,25,26}\text{Mg}$ at 90-150 MeV..... (36)

2-17 High Spin States of ^{55}Fe	(38)
2-18 Determination of Side Feeding Intensity by γ - γ Coincidence Data Analysis.....	(39)
2-19 A Study of Side Feeding of Residual Nuclei from ^{30}Si (^{28}Si , α xnp)...	(41)
3. Nuclear Chemistry and Radio-Chemistry	
3-1 The Decay of ^{248}Es	(45)
3-2 Charge Distribution in the 14.7 MeV-Neutron-Induced Fission of ^{232}Th , Independent Yields of Isotopes of Rh, Ag and Sb.....	(46)
3-3 The Decay of ^{250}Fm	(47)
3-4 Mass Distribution in 14.7MeV-Neutron-Induced Fission of ^{232}Th	(48)
3-5 The Thermochromatographic Investigation of ^{204}Tl with Air Carrier Gas.....	(49)
3-6 Treatment of Waste Water for Zinc Coatings.....	(51)
4.Applications of Nuclear Technique	
4-1 Crude Petroleum Water Content Monitor.....	(55)
4-2 The Pore Size Measurement of Nuclear Track Microporous Membrane by Flowing Rate Method.....	(56)
4-3 The Elementary Research on the Possibility for the Element Content Determination in Archaeological Samples Using 14MeV Neutron Ac- tivation.....	(57)
4-4 Possibility of Using 2.5 MeV Neutron for Activation Analysis.....	(58)
4-5 Improvement of Wear Resistance of Magnetic Head Material by N^+ -Im- plantation.....	(59)
4-6 Modification of Tribological Characteristics of Ball-Bearing Steel 9Cr18 after N^+ Implantation	(61)
4-7 The Effect of C-Ions Irradiation on Crystallization Temperature for Amorphous $\text{Fe}_{40} \text{Ni}_{40} \text{P}_{14} \text{B}_6$	(62)
4-8 Preparation of ^{109}Cd X-Rays Source by Molecular Plating Method.....	(63)
4-9 Mössbauer Spectroscopic Analysis of the Anomaly of Specific Magne- tization Coefficient of two Kinds of Iron Ores.....	(64)
4-10 Study of the Isochronal Annealing Process for the Cold-Rolling Ni by Positron Annihilation Lifetime Technique.....	(65)
4-11 Mössbauer Spectroscopy Studies of $\text{Sm}(\text{Co Fe Zr})_{7.5}$ Alloy under the Different Heat Treatment Conditions.....	(67)
4-12 CEMS Study on N^+ -Implanted Stainless Steel-9Cr18.....	(68)
4-13 Transplantation and Improvement of the Mössbauer Overlapping Spec- trum Program.....	(70)
5. Experimental Technique	
5-1 Position Sensitive and Bragg Curve Spectroscopy Detector System.....	(73)
5-2 A Time-of-Flight Mass Spectrometer for Recoil Nuclei from α -	

Decay.....	(75)
5-3 A Bragg Curve Spectroscopy for Heavy Ion Identification.....	(76)
5-4 Preparation of Targets of Natural Uranium by Electron Method	(77)
6. 2×2 MV Tandem Electrostatic Accelerator	
6-1 Status of the 2×2 MV Tandem Accelerator.....	(81)
6-2 The Gas Stripping System of 2MV Tandem.....	(82)
6-3 An Automatic Device for Measuring Magnetic Field.....	(83)
6-4 Facility for Regenerating Molecular Sieves and Experiment of Regen- eration.....	(84)
6-5 Advance in Research of PIX Set.....	(85)
6-6 Design of an Accelerator Mass Spectrometer.....	(86)
7. HIRFL	
7-1 The Status of HIRFL.....	(91)
7-2 The Present Status of SSC Main Magnet System.....	(92)
7-3 The Present Status of the RF System for HIRFL.....	(94)
7-4 The Design and Construction of $12M^3$ Testing Vacuum Chamber	(95)
7-5 The Liquid Nitrogen Flow Diagram of the SSC for HIRFL.....	(96)
7-6 A New Surface Treatment Technology for the Vacuum Chamber of SSC	(98)
7-7 The Progress of SFC-SSC Transport Beam Line.....	(99)
7-8 HIRFL Beam Transport Control System	(100)
7-9 The Experiment of Controlling Power Supplies of Correcting Magnets	(101)
7-10 The Installation and Adjustment of the Magnet System of SFC	(102)
7-11 The Preparation of GYS-500/25 Stabilized DC Power Supply	(103)
7-12 Manufacturing and Installation of RF Cavity for SFC	(104)
7-13 The Vacuum Test of the RF Cavity of SFC	(105)
7-14 Microcomputer Control for SFC Beam Acquisition System.....	(107)
7-15 The Microcomputer Control for the Extraction System in SFC	(108)
7-16 Bench Test of Cold-Cathode PIG Source and Application of Rotated Cathode	(109)
7-17 Pulsed Magnets for the Time Sharing of the GANIL Beam	(111)
8. Experimental Terminal Equipments of HIRFL	
8-1 Preliminary Plan of HIRFL Experiment Hall	(115)
8-2 Progress of On-Line Isotope Separator	(116)
8-3 An Analyser Magnet of On-Line Isotope Separator.....	(117)
8-4 The Design and Preliminary Test of the Hollow Cathode Ion Source Used for ISOL	(118)
8-5 A Device for the Measurement of Magnetic Field	(119)
8-6 The Experimental Setups for the Research of Atomic Physics on SSC	(120)
8-7 A Large Area Position Sensitive IC Experimental Terminal	(121)
8-8 In-Beam γ Experimental Setup	(123)

Large Spherical/Cylindrical Scattering Chamber for General Purpose	(124)
8-10 A Large Dynamical Range and Multi-Stack Telescope Detector	(125)
8-11 The Irradiation Equipment at HIRFL	(126)
8-12 The Rapid chemical Separating Equipment	(128)
8-13 Progress in the TOF System Project for Heavy Ion Research	(129)
9. Computer	
9-1 Two Computer Programs for Decay Curve Analysis	(133)
9-2 Progress on Computer Application	(134)
9-3 A Fitting Program for Mössbauer Spectrum with Controllable Parameters	(135)
10. Radiation Protection	
10-1 Dependence of Neutron Dose Equivalent on Intensity of Deuteron	(139)
10-2 A Summary of Radiation Safety at K-600 Neutron Generator	(140)
11. Appendix	
11-1 International Scientific Exchanges in 1985	(143)
11-2 Publications	(146)

1. Theoretical Nuclear Physics

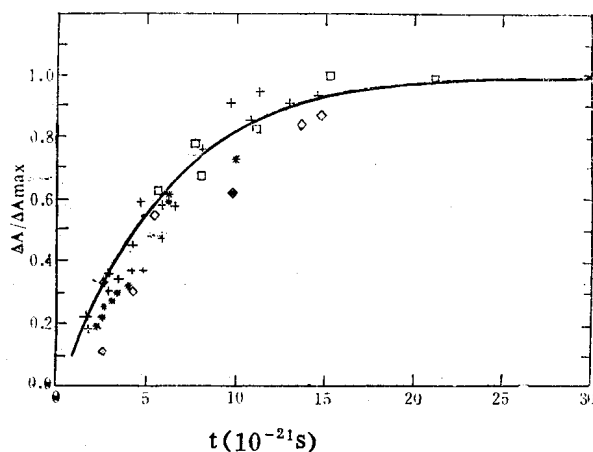
1-1 MASS DRIFT IN HEAVY ION REACTION

Ge Lingxiao Shen Wenqing Liu Jianye Wu Guohua

A simple model by which the mass drift can be expected in heavy ion reaction is suggested. The drift of average value of mass distribution with increasing dissipation energy is very small because large damping effect associated with the degrees of freedom of mass hinders the driving potential in the process of energy equilibration while in the process of fast fission the drift of mass distribution increases rapidly and reaches the equilibration which comes from the effect of driving force. Fig. 1 shows the results of $\Delta A / \Delta A_{\max}$ ($\Delta A = A_p - \langle A \rangle$, $\Delta A_{\max} = (1/2)(A_p - A_t)$) as a function of interaction time in which the results extracted by experiments were compared with calculation results based on the solution of Langevin equation²⁾ including the damping associated with the degrees of freedom of mass and driving forces.

The competition between the damping and driving force with interaction time is not clear for us but simple estimation in the two specific cases in which the driving force has been neglected or the driving and damping force have same magnitude supports the idea above.

In Fig. 1, the results extracted by experiments¹⁾ for ^{238}U induced reactions on ^{32}S (\square), ^{40}Ca (\diamond), ^{48}Ca ($+$), Zn ($*$), ^{58}Fe (\times) and ^{64}Ni (\bullet) are shown, the solid curve is the calculated result which seems to follow a general curve for the different reactions.



References

- 1) W. Q. Shen et al., to be submitted to Phys. Rev. Reports.
- 2) S. Chandrasekhar, Rev. Modern Phys., 15 (1943) 1.

1-2 MASS DISSIPATION PROCESS IN HEAVY ION COLLISIONS

Li²Junqing Zhu Jieding* Liu Jianye

The lack of mass drift towards symmetry at low TKEL in heavy ion collisions is of great interests recently, the transport theory thus faces a challenge for its conclusion under the action of a driving force during the collisions. The solution of Fokker-Planck equation, however, is analytical in the usual cases¹⁾ which is based on an approximation of harmonic oscillator potentials. The solution can not describe any quantity which is sensitive to the details of the dynamical potential. In this work the master equation is solved numerically. The distribution function $P(A_1, E^*, t)$ which gives the probability of finding A_1 nucleons in fragment 1 at time t and at the excitation energy E^* is calculated. The transition probability $W(A_1, E^*; A_1, E^*)$ is evaluated by means of statistical spectral method²⁾. Only one nucleon transition is taken to be important. The N/Z ratio is considered to reach equilibrium very promptly. The liquid-drop energy including shell effect in driving potential is calculated according to Ref.³⁾. The energy loss is treated classically.

The calculation for $^{86}\text{Kr} + ^{166}\text{Er}$ is carried out. The mean charge $\langle Z \rangle$ of fragment 1 as a function of TKE is shown in Fig. 1. There is no obvious drift for $\langle Z \rangle$ until TKEL raises to 100 MeV, below it the excitation energy is too small to create a sufficient active valence space to supply considerable element diffusion and drift (when $\sigma_A^2 = 7.585, \sigma_Z^2 = 1.142$). When TKEL exceeds 100 MeV $\langle Z \rangle$ is drifted faster than data. It may be due to the defect of the model but it must be pointed out that a very long computer time restricts the adjustment of parameters. If we reduce the strength of interaction potential so as to reduce the transition probability, $\langle Z \rangle$ would fit the data better.

To summarize, by taking the details of the driven potential and the coupling of dynamical process with diffusion process into account, the diffusion model gives

(Continued on P.7)

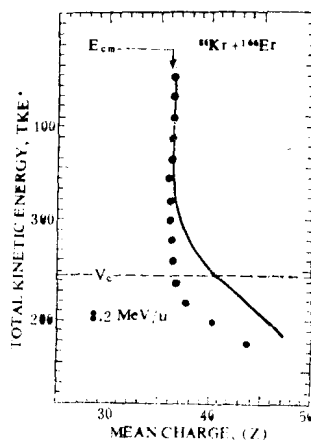


Fig. 1 Mean element distribution for $^{86}\text{Kr} + ^{166}\text{Er}$ (8.2MeV/u) reaction. The dotted experimental data is taken from Ref.4).

* Lanzhou University.

1-3 A STUDY ON DIC BY HEAVY IONS

Wang Zhenda

According to the double-well potential defined by geometric shape of asymmetric dinuclear system the Fermi-surfaces ε_F of dinuclear system will fluctuate around the top of barrier between target and projectile, which leads to the variation of neck shape, as the distance between two centers and temperature of dinuclear system KT change gradually. According to the double-well potential picture and considering the Fermi-distribution of nucleon $f_{L,h}(\varepsilon)$ filled in single particle levels of two nuclei, the quantum tunnel effect of nucleon through the barrier between two nuclei $P(\varepsilon)$ and the blocking effect due to pauli principle, the nucleon transportation number $N_L(KT, r)$ from light to heavy nucleus and $N_h(KT, r)$ from heavy to light nucleus during the average interval of nucleon collision with the wall of barrier for one time can be derived

$$N_L(KT, r) = \int_{-\infty}^{+\infty} g_{L,h}^s(\varepsilon) \cdot P(\varepsilon) \cdot f_L(\varepsilon) [1 - f_h(\varepsilon)] d\varepsilon \quad N_h(KT, r) = \int_{-\infty}^{+\infty} g_{L,h}^s(\varepsilon) \cdot P(\varepsilon) \cdot f_h(\varepsilon) \times [1 - f_L(\varepsilon)] d\varepsilon$$

where $g_{L,h}^s(\varepsilon)$ is smaller single particle levels density in two nuclei. The mass transport process can be described by Fokker-Planck-equation. There are following relations among diffusion coefficient $D(KT, r)$, drift-velocity $V_f(KT, r)$, friction coefficient $f(KT, r)$ and nucleon exchange number $N_{L,h}(KT, r)$

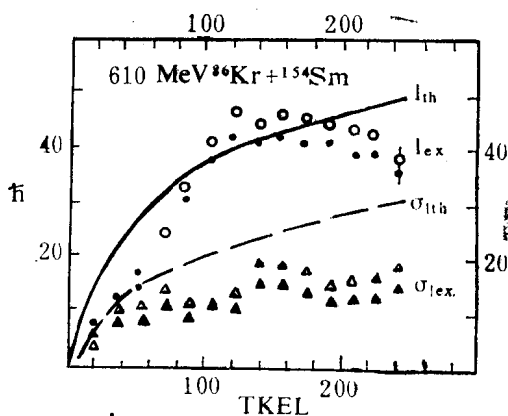
$$D(KT, r) = \frac{1}{2} [N_L(KT, r)^2 + N_h(KT, r)^2] \cdot \Delta t^{-1}$$

$$V_f(KT, r) = N_h(KT, r) - N_L(KT, r) \Delta t^{-1}$$

$$f(KT, r) = [N_h(KT, r) + N_L(KT, r)] \cdot c \cdot [\pi(a^2(c) - c^2)] \Delta t^{-1}$$

where $a(c)$ and c are parameters of geometric shape of dinuclear system described by the improved cassinian oval curve.

In heavy ion collision a part of incidence orbit angular momentum will become intrinsic angular momentum of two nuclei. Because the nucleon transfer will lead to angular momentum transfer the angular momentum diffusion coefficient $D_l(KT, r)$ and drift-velocity $V_{fl}(KT, r)$ can be derived



1-4 THE DEPENDENCE OF THE ENERGY AND MASS ON THE CONDENSATION PROBABILITY γ_β IN THE COMPLEX PARTICLE EMISSION PROBABILITY

Wu Guohua †, Miao Rongzhi ‡, Ge Lingxiao ‡, Liu Jianye

A lot of work has been done on the study of complex-particle emission probability in the pre-equilibrium statistical model. In all the work, the condensation probability γ_β is taken as a free parameter and determined by fitting the experimental data. γ_β is a constant for a given reaction. In fact γ_β is a complex function of the mass of the composite system A , the excitation energy E , the emission angle θ_β , and the energy of emission particle ε_β , i.e. $\gamma_\beta(A, E, \theta_\beta, \varepsilon_\beta)$. In the composite system, P_β nucleons distributed on P_β nearby energy levels around $(E - U/P_\beta)$ condense into the β particle with energy ε_β . For these levels the life times are shorter and the widths are larger as the energy ε_β is higher. The numbers of levels which can contribute to form the β particle with the energy ε_β are increased too. when ε_β is higher, the average energy of nucleons which condense into the β particle is higher too, the relative velocity of these excited nucleons is larger, so the collision probability is larger too. Therefore we assume that $\gamma_\beta \equiv \gamma_\beta(A, E, \theta_\beta, \varepsilon_\beta) = \gamma_\beta(A, E, \theta_\beta) \varepsilon_\beta^x$.

We calculated the energy spectra $(d\sigma/d\varepsilon)$ for 18 reactions using GEM code. Making the calculation results fit the experimental data, $\gamma_\beta(A, E, \varepsilon_\beta)$ can be extracted. Then let $\frac{d\sigma}{d\varepsilon} = \sigma_0 \sum_n W(n, \varepsilon) t_n \varepsilon^x$ and used GEM code to adjust the value of x up to the best fitting with the experimental data. The results are that for all the 18 reactions, $x = 0.425$ is the optimum value. From the latter $d\sigma/d\varepsilon$, wh-

$$D_L(KT, r) = Li^2 \left\{ \left[1 - \left(1 - \frac{1}{A_h} \right)^{N_h(KT, r)} \right]^2 + \left[1 - \left(1 - \frac{1}{A_L} \right)^{N_L(KT, r)} \right]^2 \right\} \cdot \Delta t^{-1}$$

$$V_{fL}(KT, r) = Li \left\{ 1 - \left(1 - \frac{1}{A_h} \right)^{N_h(KT, r)} \cdot \left(1 - \frac{1}{A_L} \right)^{N_L(KT, r)} \right\} \cdot \Delta t^{-1}$$

where Li is incidence orbit angular momentum. In DIC by heavy ions transport processes of the mass, charge and angular momentum can be described by Fokker-Planck equations respectively.

References

- 1) P. R. Christensen et al., Nucl. Phys., A390 (1982), 336.
- 2) R. J. McDonald et al., Nucl. Phys., A373 (1982), 54.

ich include ε^* in, we can extract $\gamma_\beta(A, E)$. γ_β is a function of $\varepsilon^{0.425}$. Using this γ_β form, the agreement between calculation and experiment is better than ever before, especially at the high energy part of energy spectra. For the same composite system the $\gamma_\beta(A, E)$ are nearly the same. When A increases the $\gamma_\beta(A, E)$ increases too. For the α -decay nucleus ^{210}Po , $\gamma_\beta(A, E)$ is larger than the other obviously.

Table 1

reactions	composite systems	excitation energy E	$\gamma_\beta(A, E, \varepsilon_\beta)$	$\gamma_\beta(A, E)$
$^{12}\text{C} (^{12}\text{C}, \alpha)$	^{24}Mg	48.7 MeV	$3.1 \cdot 10^{-4}$	$0.76 \cdot 10^{-4}$
$^{27}\text{Al} (^{12}\text{C}, \alpha)$	^{39}K	63.7 MeV	$4.2 \cdot 10^{-4}$	$1.6 \cdot 10^{-4}$
$^{nat}\text{Ca} (^{12}\text{C}, \alpha)$	^{52}Fe	66.2 MeV	$7 \cdot 10^{-4}$	$4.7 \cdot 10^{-4}$
$^{54}\text{Fe} (p, \alpha)$	^{55}Co	33.5 MeV	$4.1 \cdot 10^{-3}$	$1.0 \cdot 10^{-3}$
$^{57}\text{Fe} (p, \alpha)$		38.4 MeV	$8.7 \cdot 10^{-3}$	$2.1 \cdot 10^{-3}$
$^{56}\text{Fe} (d, \alpha)$	^{58}Co	38.9 MeV	$9.2 \cdot 10^{-3}$	$2.2 \cdot 10^{-3}$
$^{55}\text{Mn} (^3\text{He}, \alpha)$		37.9 MeV	$9.7 \cdot 10^{-3}$	$2.3 \cdot 10^{-3}$
$^{59}\text{Co} (p, \alpha)$		56.7 MeV	$8.6 \cdot 10^{-3}$	$2.1 \cdot 10^{-3}$
$^{56}\text{Fe} (\alpha, \alpha)$	^{60}Ni	57.4 MeV	$9.1 \cdot 10^{-3}$	$2.2 \cdot 10^{-3}$
$^{57}\text{Fe} (^3\text{He}, \alpha)$		58.6 MeV	$9.6 \cdot 10^{-3}$	$2.3 \cdot 10^{-3}$
$^{66}\text{Zn} (p, \alpha)$		55.0 MeV	$1.2 \cdot 10^{-2}$	$3.1 \cdot 10^{-3}$
$^{63}\text{Cu} (\alpha, \alpha)$	^{67}Ga	55.3 MeV	$1.1 \cdot 10^{-2}$	$2.8 \cdot 10^{-3}$
$^{118}\text{Sn} (p, \alpha)$		55.2 MeV	$1.8 \cdot 10^{-2}$	$4.5 \cdot 10^{-3}$
$^{115}\text{In} (\alpha, \alpha)$	^{119}Sb	55.3 MeV	$2.0 \cdot 10^{-2}$	$4.5 \cdot 10^{-3}$
$^{197}\text{Au} (p, \alpha)$	^{198}Hg	68.8 MeV	$1.2 \cdot 10^{-2}$	$3 \cdot 10^{-3}$
$^{209}\text{Bi} (n, \alpha)$		47.8 MeV	$1.3 \cdot 10^{-1}$	$3.5 \cdot 10^{-2}$
$^{206}\text{Pb} (\alpha, \alpha)$	^{210}Po	48.4 MeV	$1.2 \cdot 10^{-1}$	$3.3 \cdot 10^{-2}$
$^{207}\text{Pb} (^3\text{He}, \alpha)$		49.2 MeV	$1.2 \cdot 10^{-1}$	$3.2 \cdot 10^{-2}$

(Continued from P. 4)

the results of the lack of mass drift at low energy loss in heavy ion collision as well.

References

- 1) A. C. Merchant, W. Norenber, Preprint of GSI-81-27.
- 2) S. S. M. Wong, Sa Banhao et al., Chinese Journal of Nucl. Phys., 2(1982), 97.
- 3) W. D. Myers and W. J. Swiatecki, LBL-Report, UCRL-11980 (1965)
- 4) A. Gobbi, the preprint of GSI.

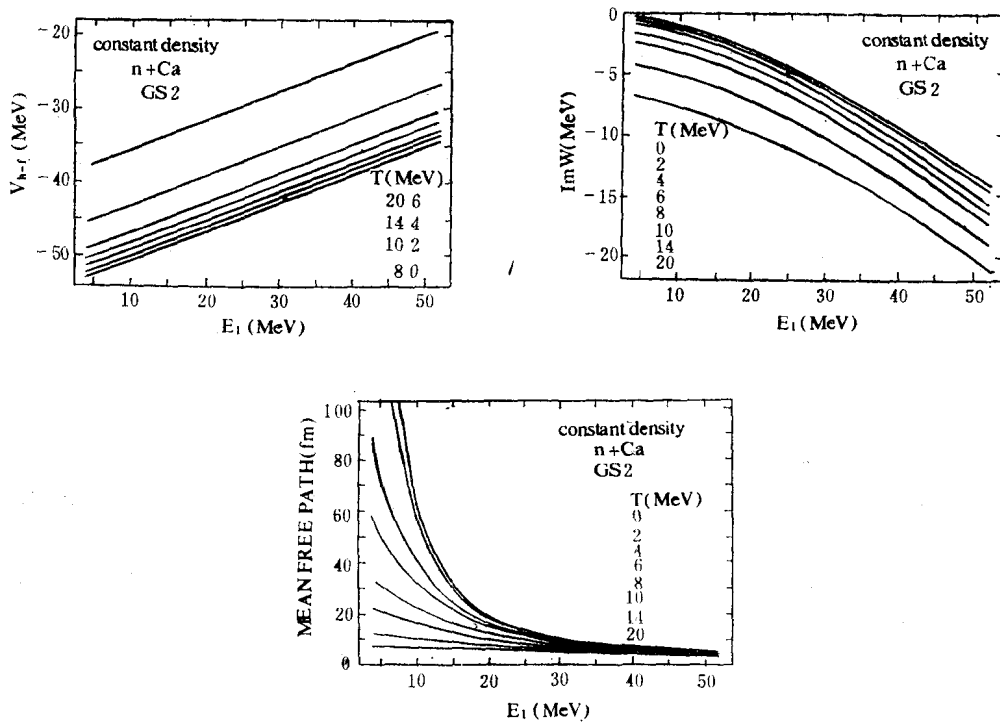
1-5 TEMPERATURE-DEPENDENT OPTICAL POTENTIAL AND MEAN FREE PATH BASED ON SKYRME INTERACTIONS

Ge lingxiao W. Norenberg Zhuo Yizhong
(GSI D-6100 Darmstadt Germany)

The understanding of the absorption of a nucleon in the nuclear medium which is characterized by the imaginary part of optical potential or by the mean free path at various equilibrium temperature is of fundamental interest in nuclear physics.

In this work, the optical potential and mean free path at finite temperatures are derived by utilizing those effective Skyrme interactions which have been tested in giving the "good" optical potential at zero temperature. Considering both the real and imaginary parts as a whole it is found that among all kinds of Skyrme interactions GS2 and SKa are the best.

The optical potentials and corresponding mean free path at various temperatures (including zero temperature) are calculated in a unified way. We have performed the calculations for symmetric and asymmetric nuclear matter and also for local density approximation. The part of results are displayed in following Fig. for constant density approximation.



1-6 STRUCTURE OF QUASI-MOLECULE IN HEAVY ION REACTIONS

Wang¹Zhengda Cao Wenqiang*

In DIC induced by heavy ions why does not the evident drift of centroid of mass (and charge) distribution along the direction of driving force (Fig. 1) appear? The reason maybe associates with the quasi-molecule structure of asymmetric dinuclear system. The nucleon exchange between two nuclei can be regarded as the motion of valence nucleons along the molecular orbits which can be not formed by only one of single particle orbit of heavy nucleus (or light nucleus). Because there is the relation in which one of single particle levels in heavy nucleus must correspond to one of single particle levels in light nucleus to form two molecular orbits

$$\psi_i(E_i) = \sum_{j=1}^2 U_{ij}(2) \varphi_j(\varepsilon) \quad (1)$$

A number of single particle levels in heavy nucleus have to remain and can not take

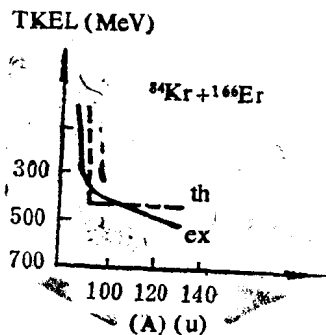


Fig. 1

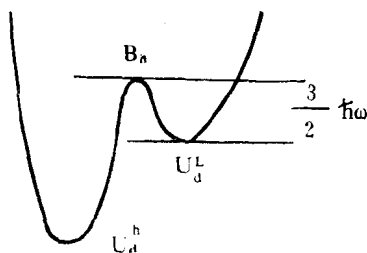


Fig. 2

part in forming molecular orbit so that the extra transportation of nucleons from heavy nucleus to light nucleus is stopped. It also likes the valence bond in diatom in which the each bond of an atom must correspond to one bond of the another. According to the picture of asymmetric dinuclear quasi-molecule how to understand the centroid of mass (and charge) distribution in quasi-fission by heavy ion drifts toward the symmetric center of two nuclei suddenly? Based on asymmetric W-type potential the deep of well of light nucleus U_d^L is smaller than that of heavy nucleus U_d^h and the height of barrier between two nuclei B_n descends as the distance of two nuclei decreases. When two nuclei close to each other and reach the critical distance at which the difference between the top of barrier and the bottom of well corresponding to light nucleus is equal to the energy of oscillator at

*Department of Modern Physics, Lanzhou University